JOURNAL OF SOLID STATE CHEMISTRY 92, 436–448 (1991)

Autocatalytic Effect in the Processes of Metal Oxide Reduction. II. Kinetics of Molybdenum Oxide Reduction

JERZY SŁOCZYŃSKI AND WALDEMAR BOBIŃSKI

Institute of Catalysis and Surface Chemistry, Polish Academy of Sciences, ul. Niezapominajek, 30-239 Kraków, Poland

Received July 16, 1990; in revised form January 2, 1991

Reduction by hydrogen of molybdenum oxide unsupported or deposited on different carriers has been studied at different reductant pressures and temperatures. It has been found that the model of the consecutive autocatalytic reaction (CAR) accounts for changes in the reaction kinetics, induced by changes in the parameters of the process as well as by the presence of supports. The model describes quantitatively the reduction of the bulk molybdenum oxide. For MoO_3 on Aerosil, the CAR model was modified by a factor related to aggregation of the intermediate product, in order to account for the additional hindrance of the reduction. © 1991 Academic Press, Inc.

1. Introduction

Kinetics and mechanism of the reduction of molybdenum oxide have been extensively studied due to their importance in the production of metallic molybdenum and to the role of MoO_3 as an essential component of many industrial catalysts for selective oxidation of olefins (*1*) and hydrodesulfurization of oil (*2*).

In the majority of papers on the reduction of MoO_3 by hydrogen or by hydrocarbons, a sigmoidal shape of the $\alpha(t)$ curves has been observed (*3–8*), which indicates that the rate of reaction goes through a maximum. Only Kennedy and Bevan (*9*) have reported the linear dependence of α versus t, but closer inspection of their results reveals that the linearity is only approximate and in reality both an increase and a decrease of the reduction rate occur.

The sigmoidal shape of the $\alpha(t)$ curves is often described by the Avrami–Erofeev equation which assumes that nucleation of the solid product of reduction is the rate limiting step. An alternative explanation of the increase in the reduction rate has been proposed by Haber and Słoczyński (*10*) for the reduction of cobalt molybdate. These authors have postulated that dissociative adsorption of hydrogen is the rate limiting step and that the acceleration of the reaction is due to an autocatalytic effect.

In many papers the reduction of molybdenum(VI) oxide to MoO_2 has been considered as a one-step reaction. Burch (*6*) was the first to suggest that Mo_4O_{11} was an intermediate product of the reduction. This hypothesis was confirmed experimentally by Ueno *et al.* (*8*), who investigated the reduction of MoO_3 in an X-ray high temperature chamber and measured the rate of formation and disappearance of Mo_4O_{11} in the course of the reduction. In the interpretation of the data the authors have not observed that the kinetics of the consecutive two-step reaction ren-

0022-4596/91 $3.00

ders possible the increase of the rate of reduction in the course of the process. The autocatalytic effect provides an additional possibility of accelerating the reaction. Recently Słoczyński (*11*), analyzing the data of Ueno *et al.*, has shown that changes in the contents of the intermediate and final products of the MoO_3 reduction, observed by these authors, may be described quantitatively by the autocatalytic effect.

In the first part of the present work, a detailed kinetic analysis of the consecutive autocatalytic reaction (CAR) model has been carried out and possibilities of the application of this model to the description of the metal oxide reduction have been shown. The criteria which allow this model to be distinguished from similar models such as the consecutive noncatalyzed reaction (the CNR model) and the consecutive reaction limited by nucleation of the reduction final product (the CNUR model) have also been formulated. In the second part of the work we concentrate on application of the results of these general considerations to the description of the kinetics of reduction of molybdenum(VI) oxide, unsupported and deposited on different supports.

2. Experimental

Molybdenum oxide was obtained by thermal decomposition of ammonium paramolybdate (APM) at 623 K followed by heating of the solid residue at 823 K for 5 hr. The preparations of molybdenum oxide on the supports were obtained by the impregnation with solution of APM, or through a surface exchange reaction with a solution of $MoCl_5$ in water-free chloroform, followed by hydrolysis of the adduct formed. After deposition of the MoO_3 precursor, the preparations were dried and calcined at 823 K for 5 hr. The supports γ-Al_2O_3 and SiO_2-Aerosil were obtained from Degussa, TiO_2 was prepared by hydrolysis of titanium(IV) butoxide followed by calcination at 673 K.

Phase composition of the samples, before and after the reduction, was determined with an X-ray method using a DRON-2 diffractometer and Cu$K\alpha$ radiation. Specific surface area was determined with the BET method using Ar or Kr as adsorbates for high and low specific surface area samples, respectively.

The rate of reduction was measured with a Sartorius vacuum microbalance connected to a standard vacuum system. Samples of 0.1–0.2 g were initially evacuated at the temperature of the measurement and at a pressure of 0.1 Nm^{-2} for 1 hr. The measurements of the rate of reduction were made in practically isobaric conditions ensured by the considerable volume of the apparatus. Mass changes of a sample were registered continuously as a function of time and the rate of reduction could be determined directly from the slope of the curve $m(t)$. Commercial hydrogen, purified by passing through a palladium filter at 573 K, was used for the reduction.

3. Results and Discussion

3.1 Characteristics of the Preparations

Characteristics of the preparations investigated are given in Table I. XRD analysis has shown the presence of crystalline molybdenum oxide in all samples containing Aerosil irrespective of the method of their preparation. For γ-Al_2O_3 and TiO_2 supports, the surface exchange with the $MoCl_5$ solution yields a "surface" MoO_3 which is not detected with the X-ray diffraction, whereas impregnation with the APM solution leads to preparations containing the crystalline MoO_3.

The preceding results agree with a known fact that the surface exchange with $MoCl_5$ leads to the formation of isolated molybdenum–oxygen polyhedra (*12*). The stronger its interaction with the support surface, the higher the stability of the molybdena layer thus obtained. This interaction is significant

TABLE I

PREPARATION METHODS, COMPOSITION, AND SURFACE AREA OF MoO_3 PREPARATIONS

Symbol	Support	Preparation method	Composition wt% of MoO_3	Specific surface area [m^2g^{-1}]		
				Total	MoO_3	Support
MoO_3 bulk	—	Decomposition of APM	100	—	1	—
SiO_2 aerosil	—	—	0	—	—	180
MoSi I		Impregnation with APM solution	11.2	141	112	146
MoSi II		Surface exchange with $MoCl_5$	14.2	119	106	121
MoSi III	SiO_2 Aerosil	Impregnation with	20.1	118	91	124
MoSi IV		APM solution	27.4	109	77	121
MoSi V			35.4	82	66	91
MoSi VI			57.2	53	38	69
γ-Al_2O_3	—	—	0	—	—	216
MoAl I	γ-Al_2O_3	Impregnation with APM solution	40.5	148	—	—
MoAl II		Surface exchange with $MoCl_5$	18.7	147	—	—
TiO_2 anatase	—	—	0	—	—	121
MoTi	TiO_2 anatase	Surface exchange with $MoCl_5$	17.9	91	—	—

for Al_2O_3 and TiO_2, whereas the molybdena layer on Aerosil is relatively weakly bound to the support and, thus, undergoes destruction during the thermal treatment, crystallizing to MoO_3 (*12–14*). The molybdenum–oxygen polyhedra were detected only on the surface of highly porous silica gels at small concentrations of molybdenum (<10% MoO_3) (*15–16*).

The specific surface area of Aerosil decreases with the increasing content of MoO_3. This indicates aggregation of Aerosil grains induced by molybdenum oxide. The decrease of the specific surface area of γ-Al_2O_3 and TiO_2 could be also due to pore filling or pore closure. The surface area of the dispersed MoO_3 can be estimated from the measurements of the rate of reduction. A detailed discussion presented later in this work shows that such estimation is valid only for molybdenum oxide supported on Aerosil. The numerical values obtained are presented in Table I. As expected, the surface area of MoO_3 decreases with the increase in the molybdenum content. The molybdena dispersion in preparations on alumina and TiO_2 obtained by the exchange with $MoCl_5$ is many times higher when compared with analogous preparations on silica.

3.2 Methods of Measurements

The X-ray diffraction pattern of the samples reduced in hydrogen in the temperature range 733–813 K reveals only the lines characteristic of MoO_2. Also the mass decrease after the full reduction of a sample corresponds to a value calculated for the transition of MoO_3 to MoO_2. The preparation MoAl(II) is the only exception, with approximately half of the molybdenum undergoing reduction according to the above stoichiometry in this case.

Thus, the reduction degree of MoO_3 was calculated as

$$\alpha = \frac{m_0 - m}{m_0 - m_\infty} = 9\left(1 - \frac{m}{m_0}\right), \qquad (1)$$

where m_0 is the initial mass of a sample, m_∞ the mass of a sample after reduction, and m the mass after time t. The factor 9 reflects the stoichiometry of the reaction. The rate of reduction was calculated from the equation

$$r = \frac{d\alpha}{dt} = -\frac{10^{-6}}{(m_0 - m_\infty)w}\frac{dm}{dt} = -\frac{9 \times 10^{-6}}{m_0 w}\frac{dm}{dt}[\text{sec}^{-1}], \qquad (2)$$

where w is the MoO_3 content (wt%), m_0 and m_∞ are given in grams, and the derivative dm/dt is determined from the slope of the curve $m(t)$ expressed in micrograms/second.

Preliminary experiments have shown that the rate of reduction, dm/dt, is proportional to the sample weight and thus $d\alpha/dt$ does not depend on the initial mass. This fact excludes diffusional hindrances in transport of the gaseous reactants to and from the reaction interface. The measurements for samples calcined at various temperatures have shown that the rate of reduction $d\alpha/dt$ is proportional to the specific surface area of MoO_3.

Figures 1a and 1b show examples of X-ray diagrams of molybdenum oxide and the preparation MoSi(II) corresponding to different stages of the reduction. The samples were reduced in the microbalance until a certain degree of reduction was attained. After removing hydrogen, the sample was cooled to room temperature and its X-ray pattern was registered. The rate of reoxidation at room temperature was found to be too low to affect the results of the X-ray analysis.

As one can see in Fig. 1., Mo_4O_{11} is formed in the initial period of the reaction and then disappears when the degree of reduction increases, with simultaneous appearance of MoO_2. These results agree with the earlier data of Ueno *et al.* who identified Mo_4O_{11} as the intermediate product of the reduction of molybdenum oxide. It can be thus concluded that, in the temperature range 733–813 K, the reduction of MoO_3 by hydrogen is a two-step consecutive reaction, following the scheme

$$\underset{(A)}{MoO_3} \xrightarrow{I} \underset{(B)}{MoO_{2.75}} \xrightarrow{II} \underset{(C)}{MoO_2}. \qquad (3)$$

Scheme (3) implies that the reduction degree α determined experimentally is a sum of two terms, related to the first and the second step of the reduction. Based on the results discussed in Part I a deconvolution of the experimental curves $\alpha(t)$ is possible and, hence, the calculation of changes in the fractional contents of all of the reactants: $x_A(t)$, $x_B(t)$, and $x_C(t)$. The change in the content of the substrate A is calculated from Eq. (I,2.8). Constant k was obtained with the aid of Eq. (I,3.13) from the initial rate of reduction determined experimentally. Values of x_B and x_C can be then calculated from relationships (I,2.3) and (I,3.1) which give the mass balance of the reactants

$$x_B = \frac{\delta}{\delta - 1}(1 - \alpha - x_A) \qquad (4)$$

$$x_C = \frac{1}{\delta - 1}(\delta\alpha + x_A - 1). \qquad (5)$$

From Eq. (I,2.3), $\delta = 4$ for the reduction of MoO_3.

Figure 2 shows an example of the deconvolution of the $\alpha(t)$ curve obtained for the reduction of molybdenum oxide by hydrogen at 813 K and at hydrogen pressure of 27.2 kNm^{-2}. Contents of the respective reactants determined with the X-ray method are marked with symbols. A very good agreement between experimental and calculated values confirms once again the fact that the MoO_3 reduction proceeds according to Eq. (3) and, hence, that Mo_4O_{11} is the only intermediate product.

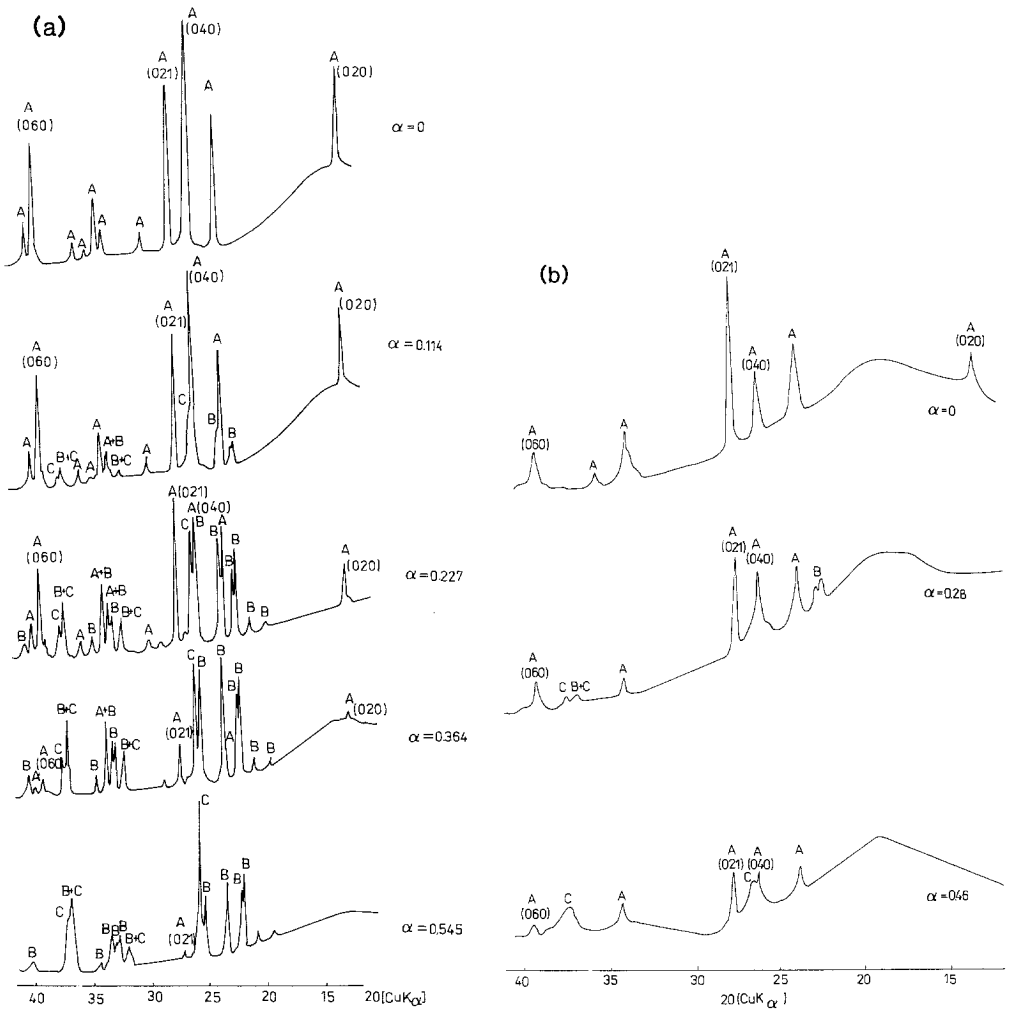

FIG. 1. (a) X-ray patterns of MoO_3 reduced in hydrogen. A, MoO_3; B, Mo_4O_{11}; C, MoO_2. (b) X-ray patterns for MoO_3 supported on silica (MoSiII) reduced in hydrogen. *A*, MoO_3; *B*, Mo_4O_{11}; *C*, MoO_2.

The deconvolution procedure may be also helpful in calculation of the kinetic constants for particular steps of the reaction, since analysis of the complicated relationship $\alpha(t)$ can be replaced by examination of simpler functions $x_B(t)$ and $x_C(t)$.

3.3 Effect of the Hydrogen Pressure on the Rate of Reduction

Figure 3 shows the rate of MoO_3 reduction at 813 K as a function of the reduction degree, for different hydrogen partial pressures. The $r(\alpha)$ curves exhibit a shallow minimum at the beginning of the reaction and a marked maximum at $\alpha = 0.5$. This shape is typical of the CAR model, discussed in Part I.

As seen in Fig. 3 the initial rate of reduction is proportional to the hydrogen pressure. All the $r(\alpha)$ curves have similar shape, which points to the same values of their relative rate constants k and κ. This implies

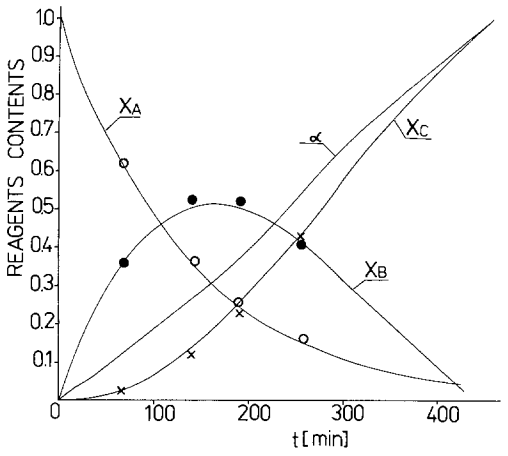

FIG. 2. Deconvolution of the curve $\alpha(t)$ for the reduction of the bulk MoO_3 in hydrogen, $T = 813$ K, $p_{H_2} = 27.2$ kNm^{-2}. *A*, MoO_3; *B*, Mo_4O_{11}; *C*, MoO_2.

that also the rate of the second reaction step is proportional to the hydrogen pressure and that the constants k and κ, which are ratios of the rate constants of the respective steps of the reaction, are independent of the reductant pressure.

Based on these results, and on the results of the preliminary experiments, the expression for the rate of reduction can be written as

$$r = \frac{d\alpha}{dt} = k_1 S p_{H_2} f(x_A, x_B, x_C), \qquad (6)$$

where k_1 is the rate constant of the first step of reduction, p_{H_2} the partial hydrogen pressure and the form of the function $f(x_A, x_B, x_C)$ depends on the kinetic model of the reaction.

In order to facilitate the comparison of data obtained under different conditions, standard values of the rate of reduction will be used further in this work,

$$R^* = \frac{1}{p_{H_2}} \frac{d\alpha}{dt} [\text{m}^2 \text{sec}^{-1}\text{N}^{-1}], \qquad (7)$$

or, when the surface area of the oxide reductant is known, the specific standard rate of reduction will be used:

$$R = \frac{1}{S p_{H_2}} \frac{d\alpha}{dt} [\text{gsec}^{-1}\text{N}^{-1}] \qquad (8)$$

When the R/R_0 ratio is considered, either of the two quantities can be used.

The linear dependance of the rate of MoO_3 reduction on the hydrogen pressure points to the dissociative adsorption of hydrogen, or the surface reaction of the atomic hydrogen with oxygen, as the possible rate determining steps of the reaction. In the second case, however, the reduction rate should be proportional to $p_{H_2}^{1/2}$. Since the rate is in fact proportional to p_{H_2}, the dissociative adsorption of hydrogen seems to be the rate determining step. This conclusion, together with the preceding observations that the reaction proceeds in the two steps with Mo_4O_{11} as the intermediate product, allow one to conclude that the reduction of MoO_3

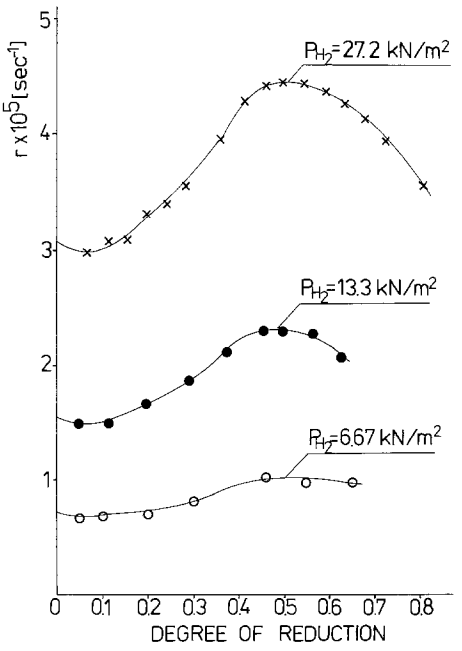

FIG. 3. Experimental curves $r(\alpha)$ for the reduction of MoO_3 at 813 K, at various hydrogen pressures.

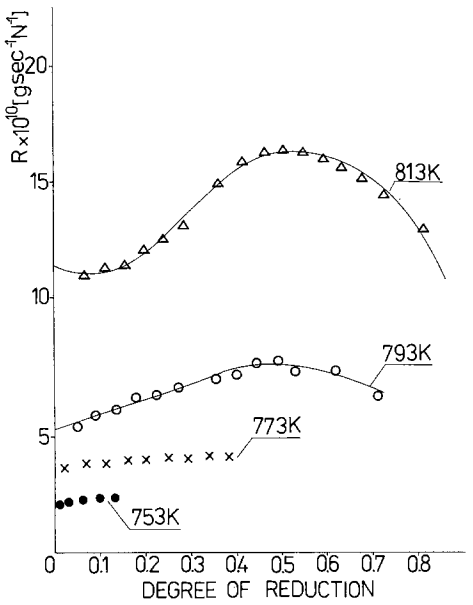

FIG. 4. Curves $R(\alpha)$ for the reduction of MoO_3 at various temperatures. Solid lines correspond to $R(\alpha)$ calculated according to the CAR model for $n = 2/3$ and for the following k i κ constants: 793 K, $k = 0.89$, $\kappa = 0.22$; 813 K, $k = 1.00$, $\kappa = 0.11$.

fulfills the postulates of the CAR model, formulated in Part I.

3.4 Effect of the Temperature on the Rate of MoO_3 Reduction

Figure 4 shows the $R(\alpha)$ curves for the reduction of MoO_3 at different temperatures. As one can see the curves have different shape and with the increase in the temperature acceleration of the reaction is more pronounced. The $(R/R_0)_{max}$ ratio is 1.45 at 813 K, and 1.53 at 793 K and decreases rapidly with the further decrease of temperature in agreement with the data of Ueno *et al.* (*8*). It can also account for the fact that the effect of the reaction acceleration was not observed in some works.

The activation energy of the first step of the MoO_3 reduction, E_a calculated from the temperature dependance of the initial rate R_0 is 125 ± 5 kJ mol^{-1} and is slightly higher than that given by Bevan and Kennedy (*9*) (116 kJ mol^{-1}) and Ueno *et al.* (*8*) (104 kJ mol^{-1}). This difference may be due to the fact that, in both the quoted works, the integral curves ($\alpha(t)$ and x(t), respectively), were analyzed, which might have led to an averaging of the rate values. In the present study, the initial rate was obtained by extrapolating the differential curve $R(\alpha)$ obtained directly in the experiment. Moreover in both papers the errors in the determination of E_a were not given, which makes the comparison of the activation energy values even more difficult. This problem will be discussed in more detail in a separate paper.

The CAR model, with $n = 2/3$, was used to analyze the kinetic curves $R(\alpha)$ for the reduction of molybdenum trioxide. The constants k and κ were obtained from a least square fit. The results of the calculations are shown in Fig. 4 (continuous line). The comparison of the curves $R(\alpha)$ calculated for $n = 2/3$ and n = 1 shows that differences between the curves are insignificant, whereas fitting of the experimental data is slightly better for $n = 2/3$.

3.5 Effect of Support on the Reduction of MoO_3

Sets of the kinetic curves $R^*(\alpha)$, shown in Figs. 5a and 5b, depict reduction of MoO_3 deposited on different supports, carried out at various temperatures and for different content of MoO_3.

Most of the curves $R^*(\alpha)$ for the MoSi preparations show a sharp maximum for $\alpha = 0.2$ that is considerably shifted to the beginning of the reaction when compared to the unsupported MoO_3.

This indicates that the silica support brings about an increase of the constant k, i.e., an increase in the rate of the second step of the reduction. With the increase in the MoO_3 content the position of the maximum is shifted toward higher values of α, approaching thus the position characteristic of the unsupported MoO_3. The behavior of

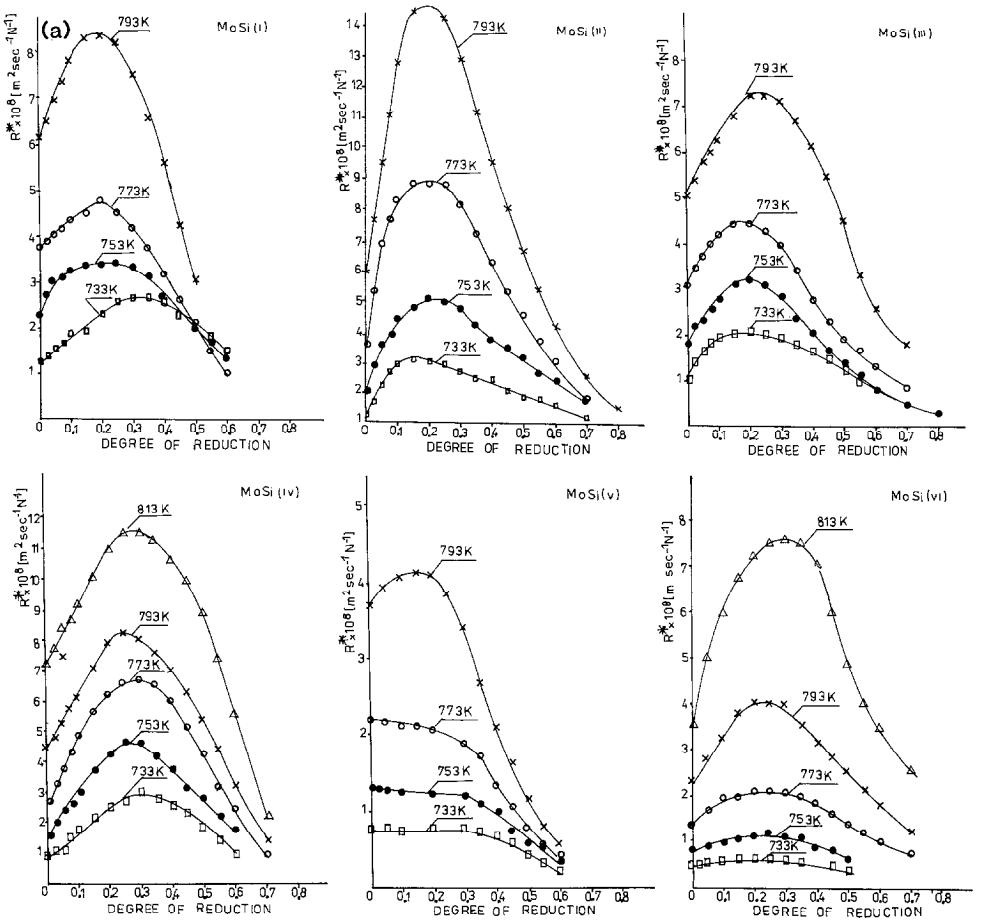

FIG. 5a. Experimental curves $R^*(\alpha)$ for the reduction of MoO_3 deposited on Aerosil.

the preparation MoSi(V) is different: a flat maximum appears only at 793 K, whereas at lower temperatures the curves $R^*(\alpha)$ decrease monotonically. This irregularity in the change of the reduction kinetics with the change in the content of MoO_3 (Fig. 5a) is due to the fact that the presence of the support affects not only the constant k, but also the value of κ, and that these two changes can have a different effect on the shape of the $R^*(\alpha)$ curves.

The analysis of the curves R/R_0 for the MoSi preparations has shown that the CAR model for $n = 2/3$ can be applied only to the initial part, up to the maximum, of the experimental curve. The declining part can be fitted, when the R/R_0 values are multiplied by the factor $\exp(-k_a \alpha + C)$, where α is the degree of reduction, and k_a and C are constants. Figure 6 illustrates the agreement between these calculations and the experimental data for the preparation MoSi(II), taken as an example.

Physical sense of multiplying by the exponential factor consists in accounting for an additional effect of hindering the second step of the MoO_3 reduction. In the CAR model, the rate of this step decreases linearly with the decreasing (with time) content of the intermediate product in the reactants

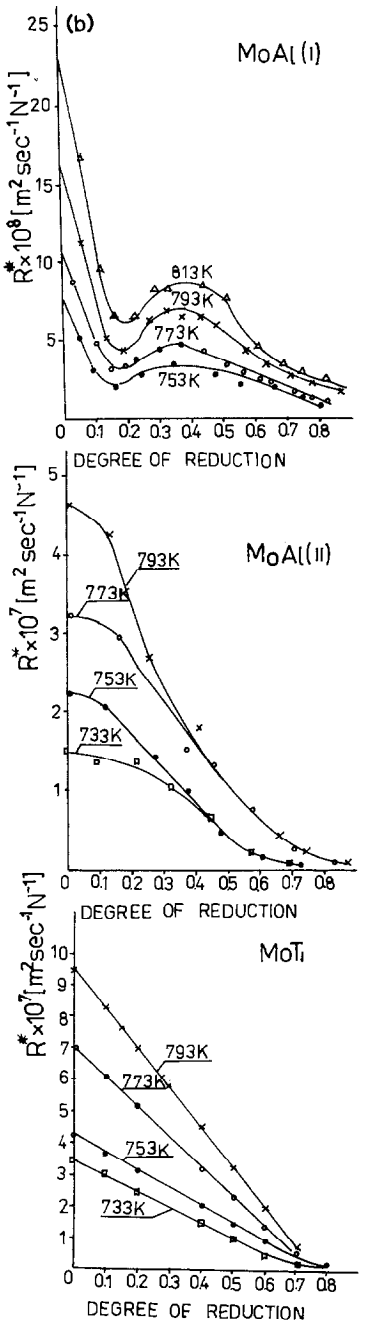

FIG. 5b. Experimental curves $R^*(\alpha)$ for the reduction of MoO_3 deposited on various supports.

mixture. The exponential factor can arise from the hindrance due to aggregation of the intermediate product B, which leads to the decrease of the reaction interface according to the equation

$$-\frac{dS_B}{d\alpha} = k_a S_B, \tag{9}$$

in which S_B denotes the specific surface area of the intermediate product and k_a the rate constant of the aggregation. The above explanation is further supported by the fact that the hindrance process does not operate from the beginning of the reaction, but starts only after the content of the intermediate product attains a certain critical level, which is a characteristic feature of many aggregation processes.

An alternative explanation of the exponential factor may be looked for in the energetic inhomogeneity of the surface of the samples. Accepting after Elovich (*17*) the linear increase of the activation energy with the degree of reduction, the effect of hindering may be ascribed to the reaction proceeding successively on the centers of higher and higher activation energy. However, the fact that the hindrance manifests itself only after a certain time for the beginning of the reaction seems to point clearly to the aggregation as the primary cause of the effect.

Alumina support has a different effect on the course of the MoO_3 reduction. The shape of the curves $R^*(\alpha)$ for the preparation MoAl(I) is very characteristic of the reduction proceeding according to the CAR model in which the first reaction step is fast and the second slow.

For comparison, we have examined also the preparations in which MoO_3 does not form a crystalline phase, but is present at the support surface in the state of the molecular dispersion. For example for preparation MoTi (Fig. 5b), the rate of reduction decreases linearly with the increase of the reduction degree. Deviations from the linearity occur only at $\alpha > 0.7$. The observed behavior can be easily explained assuming that the surface of the support is populated by identical molybdenum–oxygen centers.

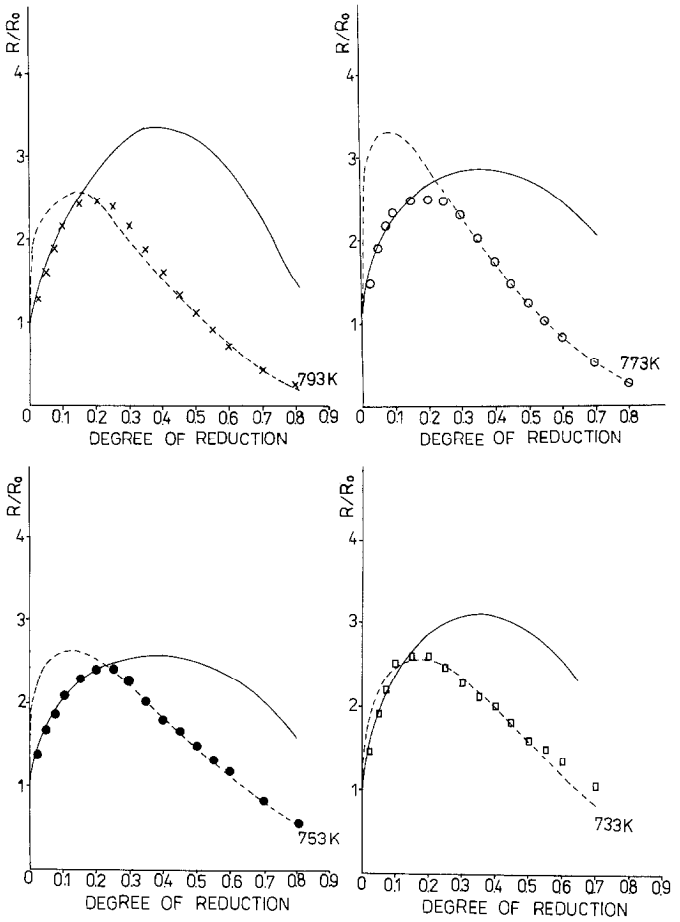

FIG. 6. Comparison of the curves (R/R_0) (α) (solid line) and (R/R_0) $\exp(-k_a \alpha + c)$ (broken line) calculated according to the CAR model for $n = 2/3$ with the experimental data for the reduction of the preparation MoSi(II) in hydrogen, at various temperatures.

Under constant pressure of a reductant, the rate of reduction is proportional to the concentration of these centers. The rate will linearly decrease as the centers are consumed in the course of the reaction.

A similar, but more complex $R^*(\alpha)$ plot is obtained for the sample MoAl(II). The rate of reduction decreases monotonically, and, in the range $0.2 < \alpha < 0.6$, depends almost linearly on the degree of reduction. However, deviations from the linearity are seen in the initial stage of the reaction, which indicates the inhomogeneity of the molybdenum–oxygen centers on the support surface.

The (R/R_0) (α) curves were used to compare more adequately the kinetics of MoO_3 reduction which differ significantly in the initial rates due to temperature changes, surface area development through the deposition on the supports, etc. A few characteristic plots of (R/R_0) (α) obtained in this work are given in Fig. 7. As seen all three types of the (R/R_0) curves possible in the CAR model are represented by (1) the monotically decreasing curves, (2) those with a

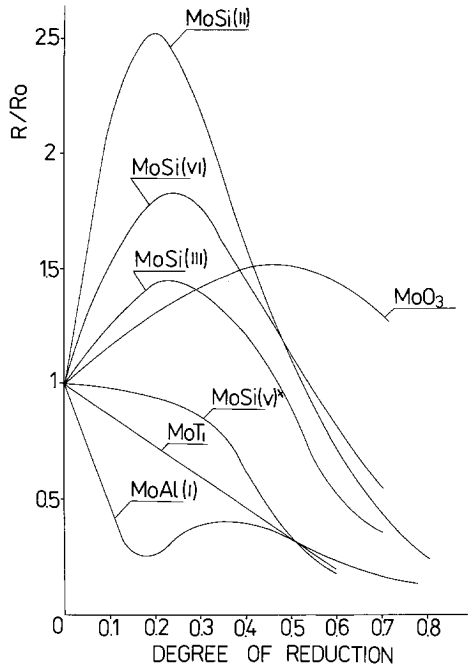

FIG. 7. Comparison of the curves (R/R_0) (α) for the reduction of unsupported MoO_3 and MoO_3 deposited on various supports.

maximum, and (3) those exhibiting a minimum and a maximum.

It can be concluded that the CAR model describes well all the changes in kinetics of MoO_3 reduction occuring when contributions from the first and second steps to the overall kinetics are varied. We can state, thus, that reduction of molybdenum trioxide is a consecutive autocatalytic reaction in which the second step is catalyzed by MoO_2. In the subsequent paper a discussion of the reduction machanism will be given, providing additional physical arguments for this conclusion and giving the comparison of the present data with those reported in the literature.

On the basis of the present results some conclusions can be, however, drawn concerning the effect of support on the reaction rate. Figure 8 shows the Arrhenius plots of the initial rates of the MoO_3 reduction by hydrogen for both bulk and supported molybdenum trioxide. Two effects are evident:

1. An increase in the rate of MoO_3 reduction by 2–3 orders of magnitude after MoO_3 deposition on the supports. The extent of this effect follows the sequence $TiO_2 > Al_2O_3 > SiO_2$, in agreement with the literature data (*13–15*). For a given support, the rate of reduction increases with the decreasing content of MoO_3.

2. Changes in the activation energy of reduction. The respective values in kilojoules per mole are 94 ± 3 for MoAl(I), 91 ± 1 for MoAl(II), and 87 ± 3 for MoTi. The activation energy for all the MoSi preparations is 128 ± 6 kJ mol^{-1} irrespective of the content of MoO_3. It is thus identical within experimental error with the value for the unsupported MoO_3.

It appears then that for the MoO_3/SiO_2 system the role of the support consists merely in an increase in the MoO_3 surface (cf. Table I) as the result of its dispersion on Aerosil, this effect being more pronounced at low MoO_3 content. The observation that silica does not change activation energy of the first step of the reduction indicates the absence of a strong interaction between molybdenum oxide and the support.

Another effect induced by the support is an increase in the rate of aggregation of the reaction intermediate product Mo_4O_{11}. The effect manifests itself in an additional hindrance of the reduction, shown in the declining part of the (R/R_0) curves. The effect is absent for the unsupported MoO_3.

The data obtained for the preparation of MoAl(I) reveal that Al_2O_3 accelerates the first step of the MoO_3 reduction more than SiO_2 and that the activation energy of the process is lower. In this case the effect of the support is not limited, as for Aerosil, merely to the development of the MoO_3 surface but consists in a strong interaction be-

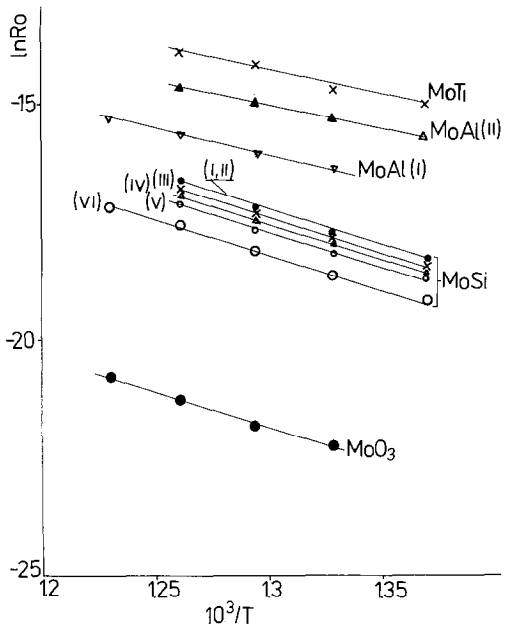

FIG. 8. Arrhenius plots for the initial reduction rate of unsupported MoO_3 and MoO_3 deposited on various supports.

tween the two components. This renders impossible a simple estimate of the specific surface area of MoO_3.

A similar situation was observed for the preparations MoAl(II) and MoTi for which a considerable increase in the initial rate of reduction (1000–2000 times when compared to the unsupported MoO_3) indicates a molecular dispersion of molybdenum on the support surface.

4. Conclusions

1. Reduction of MoO_3 both bulk and supported on SiO_2 and Al_2O_3 is a two-step consecutive reaction with Mo_4O_{11} as the intermediate product.

2. When contributions from the two steps of the reduction to the overall reaction are varied by changing the reductant pressure or the temperature, or by introducing a support, the resulting changes in the reduction rate follow predictions of the model proposed for the consecutive autocatalytic reaction (CAR).

3. The CAR model describes quantitatively the shape of the curves R/R_0 for the bulk MoO_3. For MoO_3 on Aerosil the aggregation of the intermediate product appears as an additional factor hindering the reduction process.

4. Molybdenum oxide is strongly dispersed on the Aerosil surface, but its interaction with the support is relatively weak; the support does not change the activation energy of reduction. Molybdenum oxide undergoes the molecular dispersion in the MoO_3/Al_2O_3 and MoO_3/TiO_2 systems in which strong interactions between MoO_3 and the support are present.

Acknowledgment

The technical assistance of Mrs. Z. Czuła in the reduction measurements is gratefully acknowledged.

References

1. D. J. HUCKNELL, "Selective Oxidation of Hydrocarbons," Academic Press, London/New York (1977).
2. B. C. GATES, J. R. KATZER, AND G. S. A. SHUIT, "Chemistry of Catalytic Processes," p. 390, McGraw–Hill, New York (1979).
3. PH. A. BATIST, C. J. KAPTEIJNS, B. C. LIPPENS, AND G. C. A. SHUIT, *J. Catal.* **7,** 33 (1967).
4. D. M. CHIZHIKOV, YU, E. RATNER, AND YU. V. TSVETKOV, *Izv. Akad. Nauk SSR Metal.*, **70,** 8 (1970).
5. P. RATNASAMY, A. V. RAMASWAMY, K. BANERJEE, D. K. SHARMA, AND N. RAY, *J. Catal.* **38,** 19 (1975).
6. R. BURCH, *J. Chem. Soc. Faraday Trans. I* **74,** 2982 (1978).
7. P. GAJARDO, P. GRANGE, AND B. DELMON, *J. Chem. Soc. Faraday Trans. I* **76,** 929 (1980).
8. A. UENO, Y. KOTERA, S. OKUDA, AND C. D. BENNET, *Chem. Uses Molybdenum Proc. Int. Conf. 5th,* 250 (1982).
9. M. J. KENNEDY AND S. C. BEVAN, *J. Less-Common Met.* **36,** 23 (1974).
10. J. HABER, A. KOZLOWSKA, AND J. SŁOCZYŃSKI, "Proceedings 8th International Symposium on Re-

activity of Solids Goteborg, 1976," pp. 331–335, Plenum, New York (1977).
11. J. SŁOCZYŃSKI, *React. Solids* **7,** 83 (1989).
12. G. C. BOND, S. FLAMERZ, AND R. SHUKRI, *Faraday Discuss. Chem. Soc.* **87** (1989).
13. J. LEYRER, B. VIELHABER, M. I. ZAKI, ZHUANG SHUXIAN, J. WEITKAMP, AND H. KNÖZINGER, *Mater. Chem. Phys.* **13,** 301 (1985).
14. M. J. ZAKI, B. VIELHABER, AND H. KNOTZINGER, *J. Phys. Chem.* **90,** 3176 (1986).
15. A. CASTELLAN, J. C. J. BORT, A. VAGHI, AND N. GIORDANO, *J. Catal.* **42,** 162 (1976).
16. Y. BARBOUX, *Appl. Catal.* **44,** 117 (1988).
17. V. PONEC, Z. KNOR, AND S. CERNY, "Adsorption on Solids," p. 275, Butterworths, London (1974).